

CYP450 Enzymes Effect Oxygen-Dependent Reduction of Azide-Based Fluorogenic Dyes

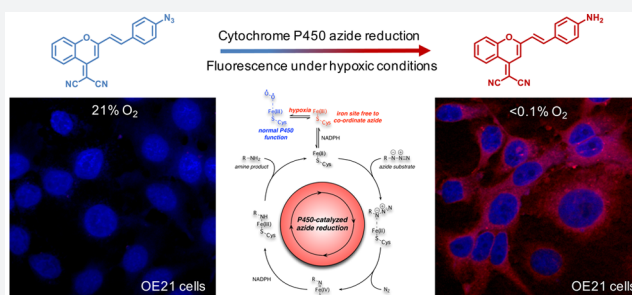
Liam J. O'Connor,^{†,‡} Ishna N. Mistry,[‡] Sarah L. Collins,[†] Lisa K. Folkes,[‡] Graham Brown,[‡] Stuart J. Conway,^{*,†,‡} and Ester M. Hammond^{*,‡}

[†]Department of Chemistry, Chemistry Research Laboratory, University of Oxford, Mansfield Road, Oxford, OX1 3TA, U.K.

[‡]CRUK/MRC Oxford Institute for Radiation Oncology, Department of Oncology, University of Oxford, Old Road Campus Research Building, Oxford, OX3 7DQ, U.K.

S Supporting Information

ABSTRACT: Azide-containing compounds have broad utility in organic synthesis and chemical biology. Their use as powerful tools for the labeling of biological systems *in vitro* has enabled insights into complex cellular functions. To date, fluorogenic azide-containing compounds have primarily been employed in the context of click chemistry and as sensitive functionalities for hydrogen sulfide detection. Here, we report an alternative use of this functionality: as fluorogenic probes for the detection of depleted oxygen levels (hypoxia). Oxygen is imperative to all life forms, and probes that enable quantification of oxygen tension are of high utility in many areas of biology. Here we demonstrate the ability of an azide-based dye to image hypoxia in a range of human cancer cell lines. We have found that cytochrome P450 enzymes are able to reduce these probes in an oxygen-dependent manner, while hydrogen sulfide does not play an important role in their reduction. These data indicate that the azide group is a new bioreductive functionality that can be employed in prodrugs and dyes. We have uncovered a novel mechanism for the cellular reduction of azides, which has implications for the use of click chemistry in hypoxia.



INTRODUCTION

Azide-containing compounds have been employed extensively in chemical biology and form the basis of many powerful tools for the interrogation of biological systems. An energy-rich functionality with high kinetic stability, azides are resistance to oxidation, amine nucleophilicity,¹ and hydrolysis under cellular conditions.² Their activation by light and use in photoaffinity labeling of an antibody was first reported by Fleet, Porter, and Knowles in 1969.³ More recently, the reaction of azides with alkynes, either in the copper-catalyzed Huisgen 1,3-dipolar cycloaddition or in uncatalyzed reactions with strained alkynes, has been the focus of much attention.⁴ Azides are not present in biological systems and alkynes are very rare, allowing selective reaction of these two functional groups in a biorthogonal manner.⁵ Consequently, azides have been employed as chemical reporters,^{1,6–14} and azide-based click chemistry has been used to facilitate imaging of biological processes, and selectively label proteins in living systems.¹⁵ Azide chemistry has also been employed for therapeutic advantage in the development of self-assembling drugs, unnatural DNA sequences, and delivery of therapeutic nanoparticles to tumors.^{16–23} In a different mode of reactivity, azide-containing dyes have been used to detect hydrogen sulfide. In particular Chang^{24–26} and Wang²⁷ have published pioneering work in this area. These compounds function through reaction between the azide and hydrogen sulfide, leading to reduction of the azide group (Figure 1).²⁸ The mechanism of this

reaction has been studied in detail by Henthorn and Pluth, and they suggest that the reduction is effected by HS^- , rather than H_2S .²⁹

Despite the reactivity of azides being extensively explored in the context of click chemistry, the behavior of azides in physiological

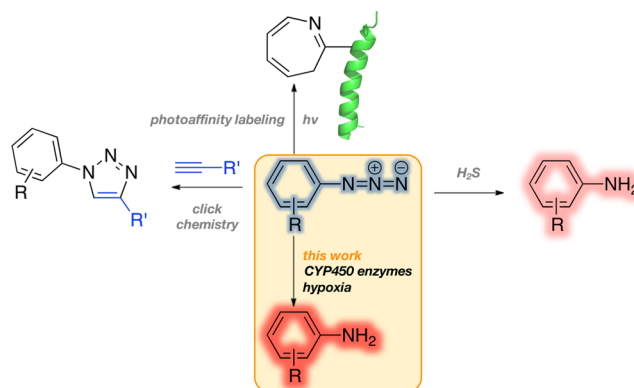


Figure 1. Azides have been employed as photoaffinity labels, in click chemistry, and as H_2S sensors. Here we report oxygen-dependent CYP450 reduction of azide-based dyes, allowing them to function as markers of hypoxia in a cellular setting.

Received: September 16, 2016

Published: December 19, 2016

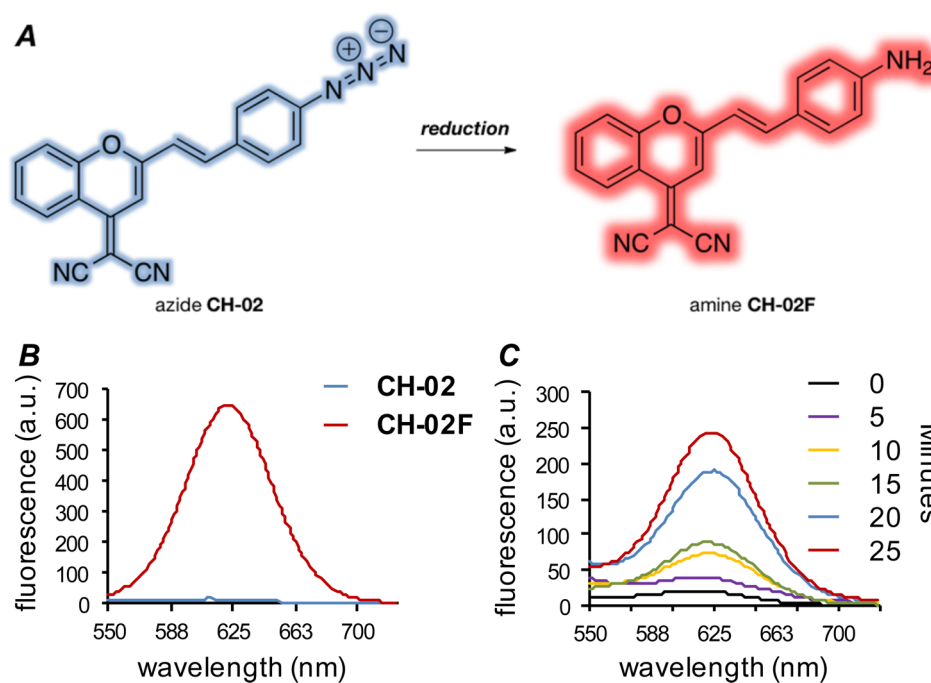


Figure 2. (A) The nonfluorescent azide CH-02 can be reduced to give the corresponding amine CH-02F, which is fluorescent. (B) Fluorescence spectra of CH-02 and CH-02F were obtained by fluorometric analysis (50 μ M, i PrOH; λ_{ex} : 515 nm). (C) CH-02 was treated with Zn/ NH_4Cl over 25 min. Fluorescence spectra were obtained every 5 min by fluorometric analysis (λ_{ex} : 515 nm).

environments is relatively poorly understood. Early investigations into the metabolism of azide-containing drugs demonstrated that mouse liver microsomes reduce electron-poor aryl azides to the corresponding amine, in the absence of air.^{30,31} Similar results were observed when the metabolism of the antiviral drug AZT,³² and a prodrug form of the antiviral drug vidarabine,³³ were investigated. These reports suggested to us that azide-containing compounds might be sensitive to oxygen-dependent metabolism, and could potentially be used as the bioreductive group in the development of oxygen-sensitive probes. We postulated that the use of azides, compared to more commonly employed bioreductive functionalities, including aromatic nitro groups,³⁴ quinones, and *N*-oxides, might confer favorable physicochemical properties for use in a cellular setting.³⁵ Therefore, we sought to validate an oxygen-sensitive bioreductive dye that would allow cellular imaging of hypoxia. Such compounds would be powerful tools for the evaluation of hypoxia in complex physiological conditions, including the tumor microenvironment and bacterial biofilms.

Here we report an azide-based fluorogenic dye that functions as a marker of hypoxia in two human cell lines, and a 3-dimensional spheroid tumor model. While steady state γ -radiolysis indicates that the azide can undergo one-electron reduction, NADPH:P450 reductase enzymes, which are responsible for the one-electron reduction of nitroaryl bioreductive compounds, had no effect on this compound. In addition, siRNA knockdown of a key component of hydrogen sulfide production indicates that this is not the primary pathway for azide reduction in this case. However, a range of CYP450 enzymes were able to reduce the azide in an oxygen-dependent manner, resulting in formation of a fluorescent amine (Figure 1). We have proposed a mechanism that explains the oxygen-dependence of the azide reduction, which to the best of our knowledge represents a novel mode of azide reduction for a wild-type enzyme in a cellular environment.

RESULTS

Chemical Synthesis and Chemical Reduction of CH-02.

To investigate the use of azides in the imaging of hypoxia we selected compound CH-02, which possesses an azide group that is conjugated to an extended π -system (Figure 2A). Previous work has shown that reduction of the azide to the amine (under other conditions) resulted in a substantial increase in fluorescence emission at a wavelength of 625 nm, and a Stokes shift of over 100 nm. Compounds CH-02 and CH-02F were synthesized using a modified version of a previously reported procedure (Scheme S1).³⁶ For synthetic details and full characterization data please see the Supporting Information. Fluorometric analysis of CH-02 and CH-02F demonstrated that CH-02F was approximately 600 times more fluorescent (λ_{ex} 515 nm; λ_{em} 625 nm) than CH-02 (Figure 2B). To confirm that the increase in fluorescence was reduction dependent, we subjected CH-02 to chemical reduction conditions that we have previously used in studies of bioreductive prodrugs.³⁷ The assay solution was analyzed using fluorimetry at regular intervals (Figure 2C), and a significant time-dependent increase in fluorescence (λ_{em} : 625 nm) was observed, consistent with the increase in fluorescence being a good indication of azide reduction.

Cellular Bioreduction of CH-02. We next determined whether CH-02 can function as a fluorogenic marker of hypoxia in a cellular setting. We initially evaluated the bioreduction of CH-02 in HepG2 cells, as they typically have high metabolic activity.³⁸ Cells were treated with CH-02 under normoxic (21% O_2) and hypoxic conditions (<0.1% O_2), and then analyzed by HPLC (Figure S1). We have defined 21% O_2 as being “normoxic” and <0.1% O_2 as being “hypoxic” in these studies; however, it is recognized that the normal O_2 concentration varies between cell types, and that normal O_2 concentrations would not be as high as 21%.³⁹ Under hypoxia (<0.1% O_2), the concentration of CH-02F increased over time; conversely, under normoxia (21% O_2), no formation of CH-02F was observed after 3 h.

In the presence of 21% oxygen, the concentration of CH-02 was constant, suggesting that no other metabolic processes were occurring (Figure 3A). This analysis was repeated in the esophageal

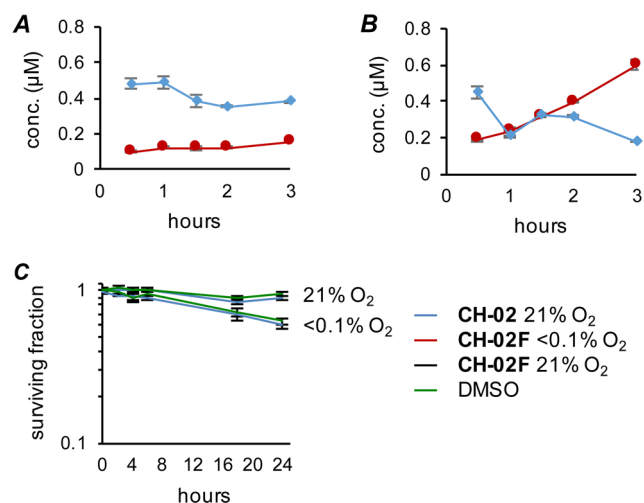


Figure 3. Compound CH-02 undergoes oxygen-dependent reduction in cells and is nontoxic. OE21 cells (0.5×10^6) were treated with CH-02 ($1 \mu\text{M}$) for 3 h under normoxic (21% O_2 , A) and hypoxic (<0.1% O_2 , B) conditions. Cells were harvested and lysed in MeCN ($50 \mu\text{L}$), and the cell lysate was analyzed by HPLC ($25 \mu\text{L}$ injections) to determine the concentration of CH-02 and CH-02F. An increase in the concentration of CH-02F was observed in hypoxia. Quantification was made using a calibration curve for CH-02 and CH-02F (a representative graph is shown, $n = 3$). (C) CH-02 (blue) is not toxic to OE21 cells relative to DMSO (green). Cells were treated with CH-02 ($1 \mu\text{M}$) under either hypoxic (<0.1% O_2) or normoxic (21% O_2) conditions for the indicated time, before replacement of media and colonies (>50 cells) allowed to form over 10 days under normoxic (21% O_2) conditions.

cancer cell line, OE21. Under normoxia (21% O_2), no formation of CH-02F was observed after 3 h (Figure 3A), whereas under hypoxia (<0.1% O_2), the concentration of CH-02F increased over time with a concomitant decrease in the concentration of CH-02 (Figure 3B). Additionally, a colony survival assay, after treatment with CH-02 under normoxic and hypoxic conditions from 0 to 24 h, revealed no observable toxicity, relative to DMSO (Figure 3C).

Fluorescence-Assisted Cell Sorting (FACS) Analysis of CH-02 Cellular Reduction. To perform a quantitative analysis of the oxygen-dependent fluorogenic qualities of CH-02, HepG2 cells were treated with compound CH-02 under normoxic or hypoxic conditions, and subsequently fluorescence-assisted cell sorting (FACS) analysis was performed. A strong induction of fluorescence under hypoxic conditions ($\sim 10\times$) was revealed, compared to normoxia (Figure 4A). A similar increase in fluorescence in response to hypoxia was observed in OE21 cells (Figure 4B).

The levels of hypoxia within tumors are known to be heterogeneous and to fluctuate dramatically.⁴⁰ Therefore, the degree of hypoxia required to reduce CH-02 to CH-02F and the stability of CH-02F once oxygen is restored are important. To investigate the broader oxygen sensitivity of the azide reduction, FACS analysis was carried out in HepG2 and OE21 cells exposed to a range of oxygen concentrations (Figure 4C,D). We observed well-defined fluorescence for each oxygen concentration investigated (21, 3, 1, 0.5, and <0.1% O_2). Furthermore, the fluorescence intensity correlated with depletion in oxygen levels.

This result demonstrates the sensitivity of CH-02 to oxygen tension. Visual inspection of the cell pellets before FACS analysis revealed a strong induction of a red color with decreasing oxygen concentration, corresponding to formation of CH-02F (Figure 4E).

To evaluate the lifetime of the fluorescent compound CH-02F, HepG2 cells were transferred to normoxic conditions after treatment in hypoxia with CH-02. FACS analysis at regular time intervals up to a period of 4 h following reoxygenation revealed that the fluorescence signal was stable (Figure 4F), indicating that CH-02F was not being degraded. This result was supported by direct treatment of cells with CH-02F under the same conditions (Figure 4G). This result demonstrated that CH-02F was stable to reoxygenation for at least 4 h, in highly metabolically active HepG2 cells.

Cellular Confocal Microscopy Using CH-02. We next evaluated whether CH-02 was suitable for use in fluorescence microscopy. HepG2 and OE21 cells were treated with CH-02 under normoxic and hypoxic conditions, and the cellular fluorescence was evaluated by confocal microscopy (Figure 5). A strong induction of fluorescence in the cytoplasm of cells exposed to hypoxia, with negligible fluorescence detected under normoxic conditions, was observed. For comparison, the experiment was repeated with the commercially available dye HypoxiTRAK (Figure S2).

Visualizing Hypoxia in a 3-Dimensional Tumor Model.

To determine whether CH-02 might be suitable for use in more intact biological settings, and to probe its permeability through multiple layers of cells, it was assessed in a spheroid 3D tumor model. For these studies the human colorectal carcinoma cell line HCT116 was selected due to its propensity for spheroid formation and growth.⁴¹ Spheroids were grown to a diameter of 500–600 μm , over 10–14 days before treatment. Initially, spheroids were treated with CH-02F under normoxic conditions, and the distribution of CH-02F was assessed by confocal microscopy after sectioning. We observed a consistent distribution of CH-02F throughout the spheroid section, suggesting that CH-02F is capable of diffusing through multiple cell layers (Figure 6A). Spheroids were then treated with CH-02 under normoxic conditions. The spheroids were disaggregated, and an increase in the concentration of CH-02F was observed when the cell lysates were analyzed by HPLC (Figure 6B).

To confirm that the reduction of CH-02 to CH-02F was occurring preferentially in regions of hypoxia (such as the center of spheroids), spheroids were treated with CH-02 and pimonidazole under normoxic conditions before sectioning and staining. A profile of fluorescence intensity for CH-02F and PIMO was taken vertically through the center of the spheroid. At the center of the spheroid an increase in fluorescence associated with the formation of CH-02F was observed, which correlated with the regions of the spheroid visualized by immunofluorescence staining for pimonidazole (Figure 6C, see Figure S3 for further examples).⁴¹ CH-02 fluorescence and PIMO staining were also shown to colocalize independent of fluorescence intensity with a Manders overlap coefficient of 0.55 (Figure S4).^{42,43} The fluorescence signal observed by confocal microscopy was confirmed to be that of CH-02F by lambda scan analysis (λ_{max} 620 nm; λ_{exc} 514 nm) as the spectrum agrees well with that previously recorded for CH-02F by fluorometric analysis (Figure 6D). These results demonstrate that CH-02 is permeable across multiple cell layers and is a marker for hypoxia in 3D models.

Investigating the Mechanism of Azide Bioreduction: Steady-State γ -Radiolysis. Bioreductive processes rely on an

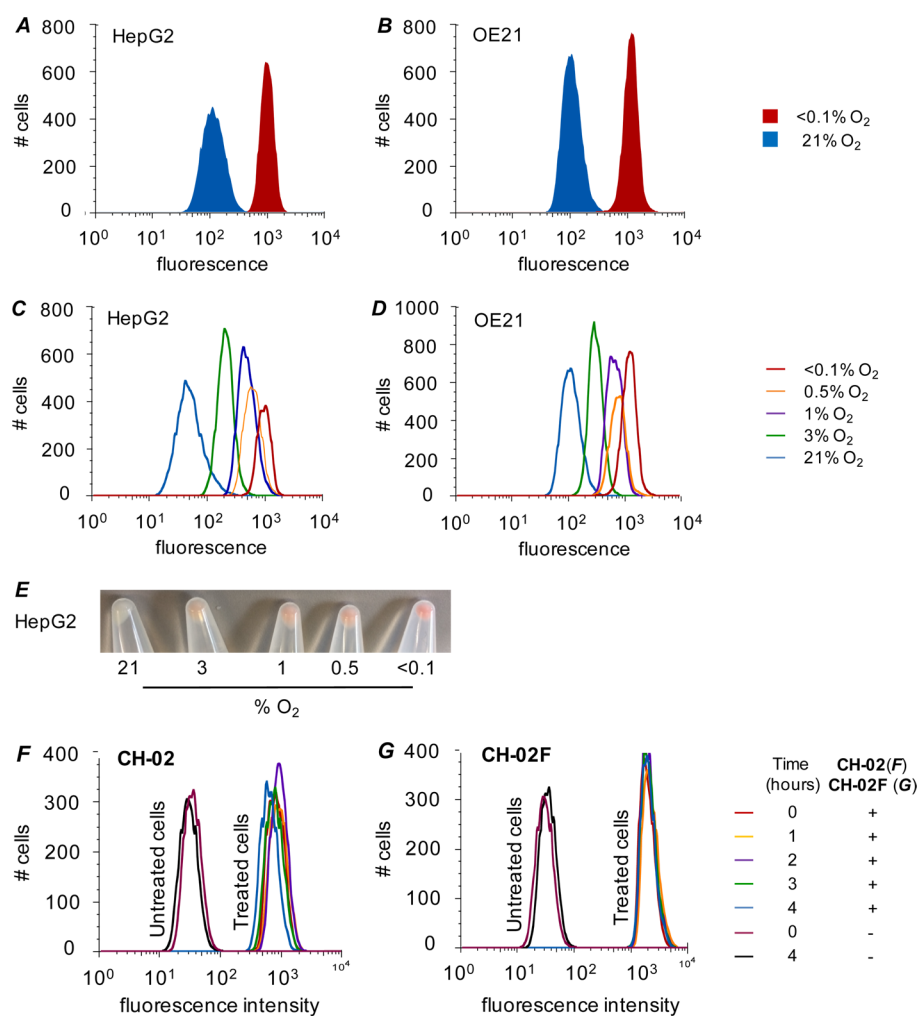


Figure 4. Compound CH-02 is suitable for determining cellular hypoxia by FACS analysis, is sensitive to a wide range of O₂ concentrations, and is stable to reoxygenation. (A) HepG2 cells were treated with CH-02 (1 μM) for 4 h under normoxic (21% O₂) and hypoxic (<0.1% O₂) conditions. A 10-fold increase in fluorescence from normoxia to hypoxia was observed by FACS analysis. (B) OE21 cells were treated as in panel A. A 10-fold increase in fluorescence from normoxia to hypoxia was observed by FACS analysis. (C) HepG2 cells were treated with CH-02 (1 μM) under the oxygen concentrations shown for 16 h: 21%, 3%, 1%, 0.5%, and <0.1%. An inverse correlation between oxygen concentration and cell fluorescence was observed by FACS analysis. (D) OE21 cells were treated as in panel C. An inverse correlation between oxygen concentration and cell fluorescence was observed by FACS analysis. (E) HepG2 cells treated as in panel C were pelleted and photographed. An accumulation of red color that corresponds to CH-02F is visible. (F) HepG2 cells were treated with CH-02 (1 μM) under hypoxic (<0.1% O₂) conditions for 4 h. Cells were then reoxygenated, and the cell fluorescence was analyzed by FACS at regular time points. (G) HepG2 cells were treated as in panel D with CH-02F (1 μM). The fluorescence observed is stable over the times shown.

enzyme-mediated process for oxygen-dependent reduction. The hypoxia-induced enzymes typically function through sequential single-electron transfers to a reducible moiety, for example, a nitro group, which is initially reduced to a nitro radical anion.³⁵ Under normoxic conditions these preliminary radicals are oxidized back to the nitro group in a process of futile cycling, which prevents further reductive steps. In the absence of oxygen, the radical undergoes further, irreversible, single-electron transfers resulting in activation of the prodrug under hypoxic conditions.⁴⁴ Steady-state γ -radiolysis can be used to produce reducing radicals at controllable dose rates, and is therefore an effective model for probing the mechanism of single-electron-mediated bioreductions.^{45–47} Consequently, this technique has been widely used to evaluate whether reductions can occur via a sequential one-electron transfer mechanism.^{48,49} To evaluate whether the azide functionality of CH-02 can be reduced by single-electron transfers, a solution of CH-02 was irradiated (14 Gy/min) under anaerobic conditions, and aliquots were

taken at regular time intervals. Subsequent HPLC analysis enabled determination of the concentrations of CH-02 and CH-02F with time (Figure 7). Fluorescent CH-02F formed in a dose-dependent fashion, and corresponded to a comparable depreciation in the concentration of CH-02, showing that CH-02F formation results directly from reaction of CH-02 with the initiating isopropanol radical. Isopropanol radicals are formed in N₂O-saturated solutions with a *G* value of 0.67 μM/Gy,⁵⁰ approximately 2-fold faster than the rate at which CH-02F is formed, suggesting that the azide in CH-02 can undergo two sequential single-electron reduction steps to form CH-02F.

Investigating the Microsomal and Enzymatic Mechanism of Azide Bioreduction of CH-02. Having determined that CH-02 is sensitive to reduction by sequential single-electron transfers, we proceeded to evaluate the biological mechanism of CH-02 reduction. Previous reports suggest that electron-deficient azide compounds undergo oxygen-dependent reduction to the corresponding amine in the presence of mouse

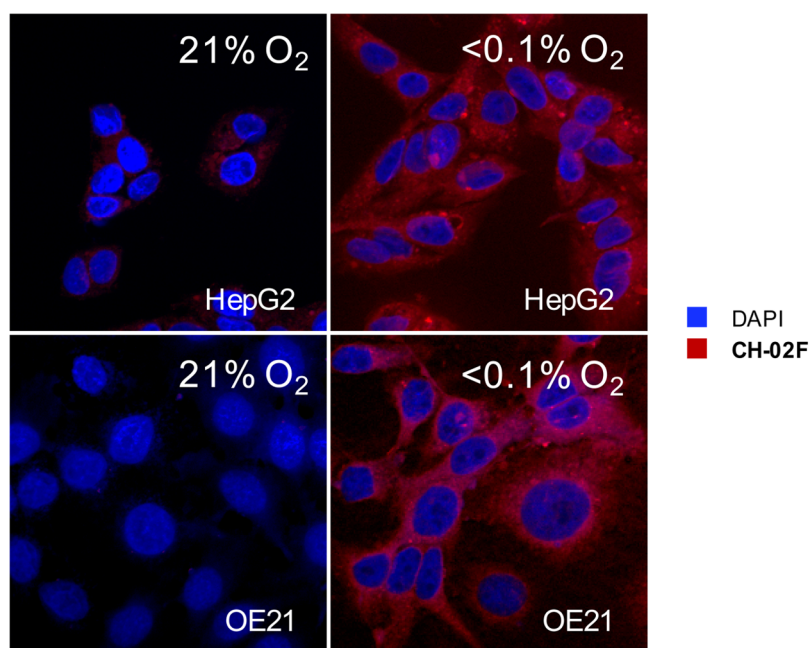


Figure 5. Compound CH-02 is suitable for determining cellular hypoxia by confocal microscopy. HepG2 and OE21 cells (as shown) were treated with CH-02 ($1 \mu\text{M}$) under normoxic ($21\% \text{O}_2$) and hypoxic ($<0.1\% \text{O}_2$) conditions for 4 h. An increase in fluorescence (red) from normoxia to hypoxia was observed by confocal microscopy. DAPI (blue) was used as a nuclear stain.

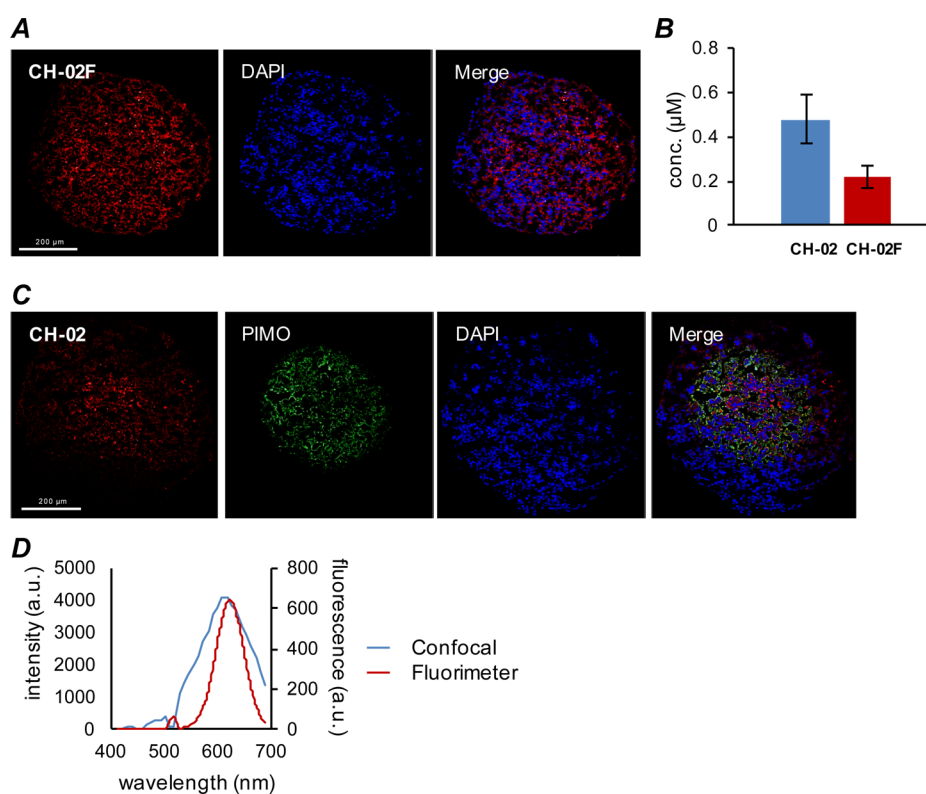


Figure 6. Compound CH-02 is suitable for evaluating hypoxia in 3D models. (A) HCT116 spheroids were treated with CH-02F ($20 \mu\text{M}$) for 8 h, fixed, and sectioned. Clear permeation of the compound throughout the spheroid was observed using fluorescence (red) confocal microscopy. As a comparison, DAPI (blue) was used as a nuclear stain. (B) Disaggregation and cell lysate analysis by HPLC ($25 \mu\text{L}$ injections) of spheroids (9 spheroids per lysate) treated with CH-02 ($20 \mu\text{M}$) for 8 h revealed formation of fluorescent CH-02F, resulting from in-cell reduction of CH-02. Quantification was made using a calibration curve for CH-02 and CH-02F. (C) Spheroids were treated with CH-02 ($20 \mu\text{M}$) and pimonidazole (PIMO) ($40 \mu\text{M}$) for 8 h, fixed, and sectioned. Pimonidazole binding was determined by immunofluorescence. Fluorescence was visualized by confocal microscopy, and DAPI was used as a nuclear stain (a representative image is shown, $n = 5$). The appearance of CH-02F, resulting from in-cell CH-02, coincides with the area of hypoxia indicated by pimonidazole staining. (D) Fluorescence spectra were obtained by confocal microscopy analysis of sections treated with CH-02, and compared to the fluorescence spectra of CH-02F obtained by fluorimetry.

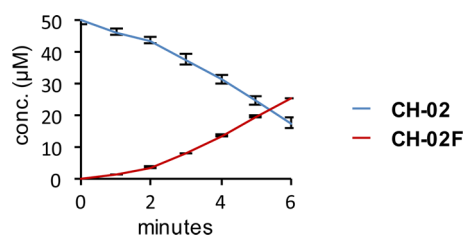


Figure 7. Compound CH-02 can undergo reduction by sequential single-electron transfers. A solution of CH-02 (50 μM) in $^i\text{PrOH}/4\text{ mM KH}_2\text{PO}_4$ (1:1, pH 7.4) buffer was irradiated (14 Gy/min) over 6 min under an anaerobic N_2O atmosphere, aliquots were taken at regular time intervals, and the concentrations of CH-02 and CH-02F were determined by HPLC analysis. Concentrations are normalized to the aliquot from $T = 0$.

liver microsomes.³¹ Compound CH-02 was exposed to human liver microsomes in normoxia and hypoxia, and while no formation of CH-02F in normoxic conditions (Figure 8A) was observed by HPLC analysis, in hypoxia, efficient, time-dependent formation of CH-02F was observed (Figure 8B).

While it is possible that a number of enzymes play a role in the bioreduction of CH-02F in cells, we wished to investigate which ones play a major role in this process. Given its involvement in the bioreduction of nitrobenzyl groups,^{37,44} we first assessed whether the NADPH:P450 reductase enzymes (coexpressed with the purified CYP enzymes) effected azide reduction. Surprisingly, no formation of CH-02F was observed in either hypoxia or normoxia (Figure 8C,D), suggesting that the reduction of the azido group in CH-02 proceeds via a distinct mechanism to the nitro groups in bioreductive compounds. As human liver microsomes contain cytochrome P450 enzymes (CYP), we hypothesized that the CYP enzymes found in the microsomes could be responsible for the bioreduction of CH-02. Compound CH-02 was treated with one of five individual bacterial CYP450 enzymes (CYP 1A2, 2D6, 3A4, 2C9, 2C19), coexpressed with human NADPH:P450 reductase in the presence of 21%, 2%, or <0.1% oxygen (Figure 8E–I). Under the more severe hypoxic conditions (<0.1% O_2), each of the individual enzymes efficiently reduced CH-02, with 2D6 and 2C9 most effectively mediating bioreduction. The observed reduction was oxygen-dependent, and in the presence of 2% oxygen the reduction

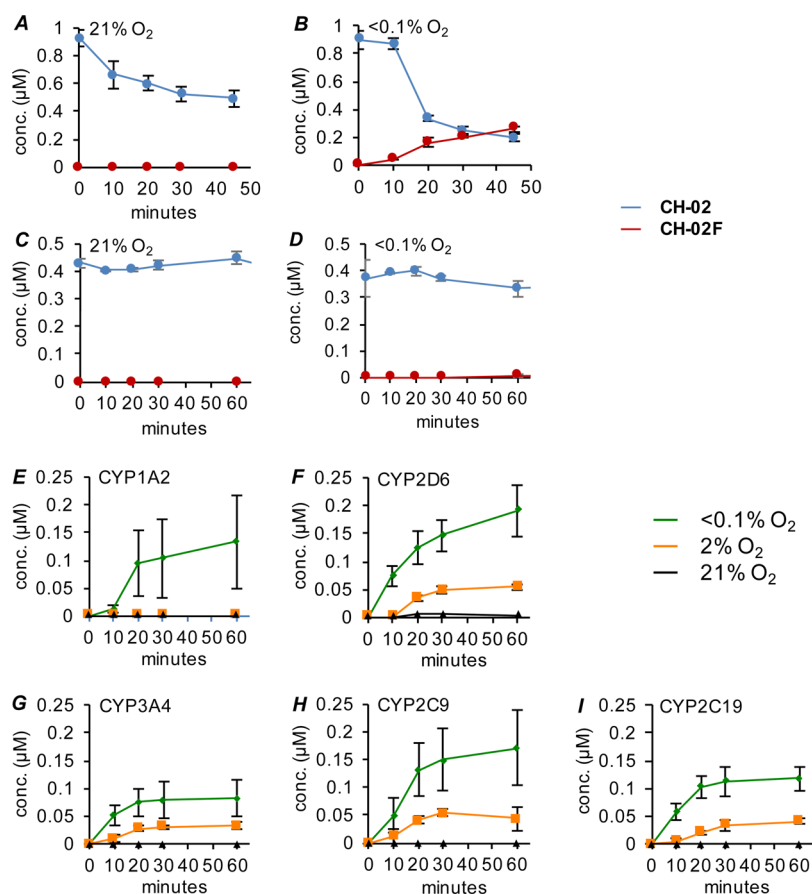


Figure 8. Compound CH-02 undergoes oxygen-dependent CYP-catalyzed reduction to fluorescent CH-02F. (A) CH-02 (1 μM) was treated with pooled human liver microsomes under hypoxic (<0.1% O_2) conditions over 45 min. Aliquots were taken as described in the Supporting Information, and analyzed by HPLC (25 μL injections) to determine the concentration of CH-02 and CH-02F. Concentrations are not scaled (a representative graph is shown, $n = 3$). (B) Normoxic (21% O_2) conditions as in panel A (a representative graph is shown, $n = 3$). (C) CH-02 (1 μM) was treated with NADPH-CYP reductases under normoxic (21% O_2) conditions over 60 min. Aliquots were taken at regular time points and analyzed by HPLC to determine the presence of CH-02F ($n = 3$). (D) Hypoxic (<0.1% O_2) conditions as in panel C ($n = 3$), showing that CH-02 is not reduced by NADPH-CYP reductases either in normoxia or in hypoxia. (E–I) Compound CH-02 was exposed to purified individual CYP450 enzymes (as shown) under normoxic (21% O_2 , black), moderately hypoxic (2% O_2 , yellow), or hypoxic (<0.1% O_2 , green) conditions. Aliquots were taken as described in the Supporting Information and analyzed by HPLC (25 μL injections) to determine the concentration of CH-02 and CH-02F. Quantification was made using a calibration curve for CH-02 and CH-02F ($n = 3$).

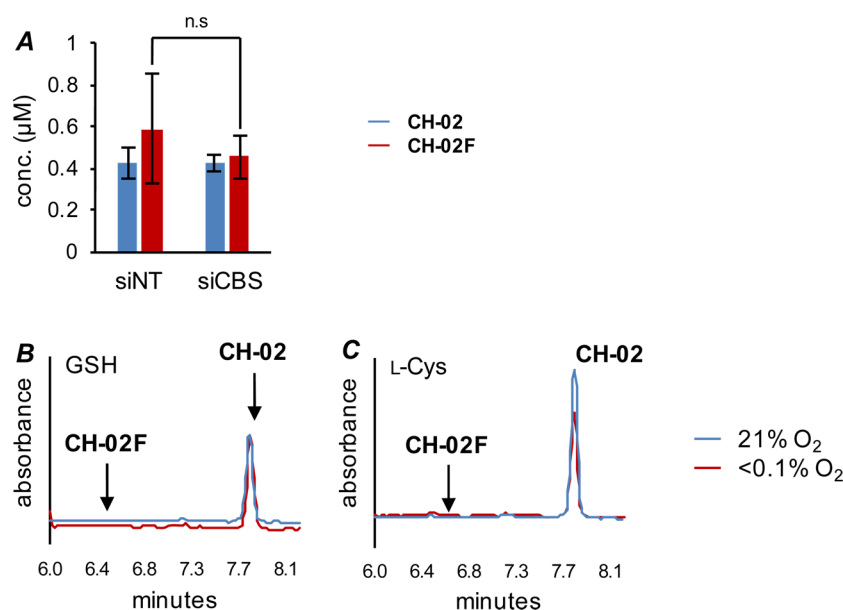


Figure 9. Compound CH-02 is stable to common cellular nucleophiles. Reduction of CH-02 under hypoxic conditions is not affected by depleted cystathionine- β -synthase (CBS) levels, a producer of H₂S. (A) OE21 cells with normal CBS levels (siNT) or depleted CBS levels (siCBS) were treated with CH-02 (1 μ M) for 4 h under hypoxic (<0.1% O₂) conditions, and the cell lysates were analyzed by HPLC (25 μ L injections) ($n = 3$), revealing no significant difference in the formation of CH-02F. (B) Compound CH-02 was treated with the cellular sulfur-containing nucleophile, glutathione (GSH), for 16 h under normoxic (21% O₂) and hypoxic (<0.1% O₂) conditions, and the reaction solution was analyzed by HPLC. The key shown applies to panels B and C. (C) CH-02 was treated with L-cysteine as in panel B. In both cases, no formation of CH-02F was observed.

efficiency was decreased by 60–75% in all cases, with CYP1A2-mediated conversion being entirely abrogated. In the presence of 21% oxygen CH-02 underwent no detectable reduction with any of the five enzymes investigated. In each case, any increase in concentration of CH-02F correlated with the appropriate decrease in concentration of compound CH-02 (Figure S4). This finding suggested that the primary pathway of CH-02 metabolism was reduction to CH-02F. The structurally distinct azide 7-azido-4-methylcoumarin was also efficiently reduced, in an oxygen-dependent manner, by CYP2D6 and CYP2C9 (Figure S4). In preliminary work, dansyl azide was observed (by LCMS analysis) to undergo reduction and demethylation when exposed to CYP2C9, CYP2C19, CYP2D6, or CYP3A4 for 24 h (Figure S5), whereas an alkyl azide underwent a competing hydroxylation reaction when exposed to the same enzymes (Figure S6). The full scope of this reaction will be the subject of further studies. However, these data suggest that the observed bioreduction is a more general phenomenon, and is not an artifact of the specific structure of compound CH-02. No upregulation of CYPs 2D6, 2C19, 2C9, or 3A4 was observed in OE21 cells after exposure to hypoxic conditions for 4 h, as determined by Western blot analysis (Figure S7). This observation indicates that the oxygen dependence of the azide reduction results from the enzymatic mechanism, rather than upregulation of enzymes in hypoxia.

Investigating the Mechanism of Azide Bioreduction: Reduction by Thiols. Compound CH-02 has previously been reported to undergo H₂S-mediated reduction in a range of *in vitro* and *in vivo* settings.³⁶ However, in this study high concentrations of NaHS were added to effect reduction, but there was no demonstration that the compound was reduced by endogenously produced H₂S. To test whether H₂S was playing a role in the observed cellular reduction of CH-02 we sought to investigate the function of the principal enzymes involved in cellular production of H₂S—cystathionine- γ -lyase (CSE) and cystathionine- β -synthase (CBS). In particular we were interested in the

function of CBS, which is a HIF-1 target and accumulates in hypoxic tissue.⁵¹ Initial studies employing chemical inhibitors of CSE and CBS were inconclusive and did not preclude off-target effects due to the promiscuous nature of the inhibitors available (Figure S8A). Therefore, OE21 cells were depleted of CBS using siRNA, and knockdown was confirmed by Western blot analysis (Figure S8B). These cells were then treated with CH-02 under hypoxic conditions, and analysis of the cell lysates by HPLC revealed no significant difference in the formation of CH-02F, relative to OE21 cells with normal CBS function (Figure 9A). In addition, compound CH-02 was stable in the presence of GSH and L-cysteine (Cys), in both normoxia (20% O₂) and hypoxia (<0.1% O₂) (Figure 9B,C), over a period of 16 h. Therefore, although we cannot rule out a role for thiols, and in particular H₂S, in the bioreduction of CH-02, we found no evidence to suggest that this is the major pathway in the systems that we have investigated.

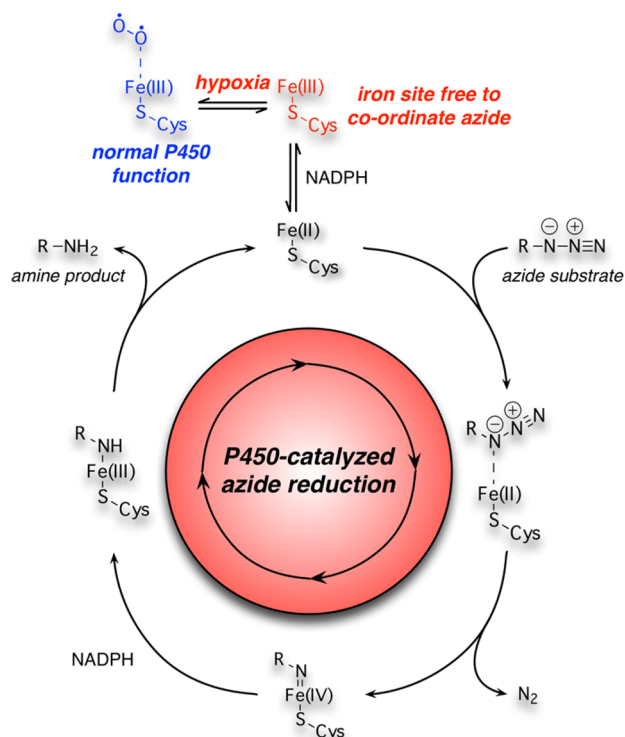
DISCUSSION

Despite the maturity of the bioreductive field, the number of functional groups that undergo oxygen-dependent reduction in a biological setting are relatively few.³⁵ The most widely used compounds contain nitroaryl groups, which have a number of drawbacks including negatively affecting the physicochemical properties of the parent compounds. Azides typically impart more favorable physicochemical properties to their parent compounds, and are commonly included in biological tool compounds. Despite the popularity of azide–alkyne click reactions, the metabolism of azides in biological settings, and in particular in hypoxia, is poorly studied. The few reports of azides undergoing reduction in a biological context prompted us to examine whether this group could form the basis of a fluorogenic dye that acts as a biomarker for hypoxia. We have shown that CH-02 undergoes oxygen-dependent reduction in HepG2 and OE21 cells, resulting in fluorescence that is suitable

for imaging by confocal microscopy in cells. The increase in fluorescence was quantified using FACS, and imaging in spheroids demonstrated that permeation of the compound would allow its use in tumors. Therefore, we conclude that CH-02 is a useful probe for the cellular imaging of hypoxia.

To understand the mechanism by which CH-02 is reduced we first conducted steady state γ -radiolysis experiments, which showed that this compound can undergo reduction through a one-electron pathway, in the absence of oxygen. However, the NADPH:P450 reductase enzymes that are responsible for the one-electron reduction of nitroaryl bioreductive compounds had no effect on CH-02 in either normoxia or hypoxia. The effective bioreduction of CH-02 in human liver microsomes led us to investigate the action of a suite of bacterial CYP450 enzymes on the compound. Surprisingly, all five of the enzymes evaluated caused rapid and oxygen-dependent reduction of CH-02. Having demonstrated the insignificant effect of H₂S on CH-02 in the conditions investigated here, we conclude that the CYP450 enzymes are likely the main route for CH-02 bioreduction in the systems examined. This observation raises the questions of the mechanism by which the azide is reduced and why this reduction is oxygen dependent. The time frame of the bioreduction indicates that these enzymes are not upregulated as part of the cellular hypoxic response, and therefore there must be another mechanism responsible for the oxygen-dependent nature of the reduction. We propose the mechanism shown in Scheme 1 for

Scheme 1. Proposed Mechanism of Bioreduction of Aryl Azides in the Absence of Oxygen by CYP Enzymes^a



^aThe azide coordinates to the heme center, and reduction proceeds via a nitrenoid intermediate.

the bioreduction of azides by the CYP450 enzymes, which is inspired by the mechanism proposed by Farwell et al.⁵² and Singh et al.⁵³ for their engineered cytochrome P450 systems. Sasmal et al. have also reported iron(III) *meso*-tetraarylporphine-based

catalysts that reduce azides.⁵⁴ In our system, under conditions of normoxia we hypothesize that the iron center is blocked by oxygen and hence the azide species is unable to bind, explaining why reduction is only observed under conditions of reduced oxygen. In hypoxia, the iron center is available for the azide to bind, forming a presumed nitrenoid species with resulting ejection of N₂. Subsequent reduction by NADPH results in the amine species being formed. To the best of our knowledge, this represents a novel mechanism for the cellular reduction of azide groups by wild-type enzymes.

In light of our results it seems that the interpretation of cellular data generated in hypoxia using azide-based H₂S-detecting dyes will require careful analysis. While we are not suggesting that H₂S/HS⁻ cannot reduce aryl azides, it seems that an alternative mechanism is available for the bioreduction of these compounds in conditions of low oxygen. This is particularly relevant for the detection of H₂S in cells with wild-type expression levels of CSE and CBS, where no exogenous NaHS is added. Our data also have wider implications for azide-based click chemistry, showing that while we think of azides as being biorthogonal, careful consideration must be given to the context of their deployment. It seems likely that attempts to employ azide-based click chemistry in a hypoxic environment would be hampered by reduction of the azide group, complicating subsequent data interpretation. Taken together, the data presented here indicate that azide bioreduction is a new avenue worthy of further exploration for the development of powerful chemical tools, including bioreductive dyes and prodrugs.

METHODS

Cell Lines and Spheroid Growth. The HepG2 (hepatic) cancer cell line was cultured in DMEM medium containing 10% FBS, penicillin (100 U/mL), and streptomycin (100 μ g/mL). The OE21 (esophageal) cancer cell line was cultured in RPMI medium containing 10% FBS, penicillin (100 U/mL), and streptomycin (100 μ g/mL). Spheroids were grown using HCT116 cells using the liquid overlay method.⁵⁵ In brief, exponentially growing cells were trypsinized and 1×10^3 cells were seeded in DMEM onto a 1% agarose-coated well of a 96-well plate. Spheroids were grown for 10–14 days until the diameter was 500–600 μ m. Medium was replaced every 2 days. With the exception of colony survival and spheroid growth, experiments were carried out with cells at 75% confluence. Cells were cultured in a standard incubator for mammalian tissue culture, maintained at 37 $^{\circ}$ C, 21% O₂ and 5% CO₂. Cells and spheroids were imaged using a Zeiss 780 confocal microscope measured using the ZEN 2012 software. All cell lines were originally obtained from the ATCC and routinely mycoplasma tested and found to be negative.

Chemical Synthesis. Details of the chemical synthesis and analytical data for the compounds described are available in the Supporting Information.

Hypoxia Treatment. Hypoxia treatments were carried out in a Bactron II Anaerobic Chamber (Shell Laboratories) or Whitley H35 Hypoxystation (Don Whitley) depending on the level of hypoxia required. For experiments at <0.1% O₂ cells were plated on glass dishes.

Fluorometric Analysis. Fluorescence spectra were obtained using a PerkinElmer LS 50 B luminescence spectrometer. Spectra were obtained from 50 μ M solutions in 2-propanol (ⁱPrOH) with an excitation wavelength of 515 nm.

Zinc Reduction. To a 50 μ M solution of CH-02 (0.9 mL) in 2-propanol (ⁱPrOH) was added aqueous ammonium chloride

(10% w/v, 100 μ L). Zinc (3 mg) was then added to the cuvette and physically shaken between obtaining fluorescence spectra at regular intervals (where $T = 0$ refers to the spectrum obtained before addition of zinc).

Steady-State γ -Radiolysis. A solution of CH-02 (50 μ M) in 1:1 v/v i PrOH and 4 mM KHPO_4 buffer (pH 7.4) was made. The solution (1 mL) was transferred to a glass HPLC vial (2.5 mL) and degassed for 15 min with N_2O gas. A $T = 0$ aliquot was taken. The vial was irradiated for 6 min at 14 Gy/min, in a cesium-137 GSR D1 irradiator (Gamma-service Medical GmbH, Leipzig, Germany), and aliquots (50 μ L) were taken at minute intervals. The aliquots were analyzed by HPLC, making injection volumes of 10 μ L.

NADPH Reductase/Microsome/CYP450 Assay. Enzyme sets were used in combination with an NADPH-regenerating system, and the assay was carried out at a CH-02 concentration of 1 μ M. Further protocol details can be found in the [Supporting Information](#). Vials were transferred to an aerobic incubator (37 $^\circ\text{C}$) or Bactron II Anaerobic Chamber. Aliquots (50 μ L) were taken at different time points and injected into MeCN (50 μ L). Protein debris was removed by centrifugation and the solution analyzed by HPLC at 420 nm, making injection volumes of 25 μ L.

HPLC Analysis. HPLC (Waters 2695 system) comprised an RPB column (5 μm , 100 mm \times 3.2 mm, 35 $^\circ\text{C}$). Separation was achieved at a flow rate of 0.5 mL/min with a gradient of 30–95% acetonitrile in 10 mM formic acid over 6 min, returning to starting conditions over 0.1 min. Detection used a photodiode array spectrophotometer (Waters 2996) and a mass spectrometer (Waters Micromass ZQ mass spectrometer). Injections of 25 μ L were made.

Flow Cytometry. Cells were harvested and treated with trypsin for 5 min at 37 $^\circ\text{C}$, and the trypsin was removed by centrifugation at 250g. The cells were then fixed with 4% PFA for 15 min. For fluorescence analysis the fixative was removed by centrifugation at 250g, and the cells were suspended in PBS. The samples were run on a Becton-Dickinson FACScan. Analyses were carried out using Flowjo (Treestar, Ashland, OR 97520).

Clonogenic Assay. Cells were seeded and treated with CH-02 (1 μ M) under 21% and <0.1% O_2 for 4 h. Colonies (>50 cells) were left to form for 10 days and visualized with methylene blue stain (70% methanol in PBS, 1% methylene blue (Fisher BioReagents)).

Western Blotting. Cells were lysed in UTB (9 M urea, 75 mM Tris-HCl pH 7.5, and 0.15 M β -metcaptoethanol), and each sample was sonicated for 20 s. Antibodies used were cystathionine- β -synthase (Sigma-Aldrich), HIF-1 α (BD Biosciences), and β -actin (Santa Cruz).

RNA Interference. Human CBS siRNA (ON-TARGETplus SMARTpool, Dharmacon) or RNAi negative control (ON-TARGETplus, Dharmacon) was transfected into cells using DharmaFECT 1 at a final concentration of 50 nM. 0.15×10^5 cells/well were seeded in 6 well plates the day before the transfection. Cells were incubated with the siRNA for 16 h, the medium was replaced, and cells were incubated for 24 h, followed by treatment with CH-02 (1 μ M) at <0.1% O_2 for 4 h.

Spheroid Immunofluorescence. Spheroids were fixed in 4% paraformaldehyde at 4 $^\circ\text{C}$ for 16 h and treated with 30% sucrose (w/v, PBS) for 3 h before mounting in OCT embedding medium (ThermoScientific). Spheroids were sectioned, rehydrated in 0.1% Tween (v/v, PBS), and blocked with 1% bovine serum albumin (BSA) (w/v, PBS) for 2 h at room temperature. Sections were washed with 0.1% Tween before treatment with

pimonidazole primary antibody (Clone 4.3.11.3, Hypoxyprobe) for 2 h, washed with 0.1% Tween, and treated with Alexa Fluor 488 green secondary antibody. Sections were washed with 0.1% Tween and stained with DAPI solution (0.1 $\mu\text{g}/\text{mL}$), and the slides were mounted using ProLong Gold mounting medium (Invitrogen/Life Technologies). Slides were analyzed using a LSM780 (Carl Zeiss Microscopy Ltd.) confocal microscope.

■ ASSOCIATED CONTENT

📄 Supporting Information

The Supporting Information is available free of charge on the ACS Publications website at DOI: [10.1021/acscentsci.6b00276](https://doi.org/10.1021/acscentsci.6b00276).

Experimental procedures, ^1H and ^{13}C NMR spectra, compound purity data, and figures (PDF)

■ AUTHOR INFORMATION

Corresponding Authors

*E-mail: Stuart.conway@chem.ox.ac.uk.

*E-mail: Ester.hammond@oncology.ox.ac.uk.

ORCID

Stuart J. Conway: 0000-0002-5148-117X

Notes

The authors declare no competing financial interest.

■ ACKNOWLEDGMENTS

The authors thank Prof. Sir Jack Baldwin, Dr. Ewen Calder, Prof. Boris Vojnovic, and Prof. Luet Wong for helpful discussions. We are grateful to Dr. Michael Stratford for invaluable technical assistance. S.J.C., E.M.H., and L.J.O. thank the MRC for the award of a studentship to L.J.O. S.L.C., S.J.C., and E.M.H. thank the BBSRC (BB/L016214/1) and Novartis for studentship funding. I.N.M., S.J.C., and E.M.H. thank the MRC (MR/N009460/1) for funding. E.M.H. thanks Cancer Research UK for research funding. S.J.C. thanks St Hugh's College, Oxford, for research funding. We thank Professor Laura Herz and Dr. Juliane Gong for assistance with measuring the fluorescence lifetime of CH-02F.

■ DEDICATION

Dedicated to the memory of Jesse Moses.

■ REFERENCES

- (1) Prescher, J. A.; Bertozzi, C. R. Chemistry in living systems. *Nat. Chem. Biol.* **2005**, *1*, 13–21.
- (2) Kolb, H. C.; Finn, M. G.; Sharpless, K. B. Click Chemistry: Diverse Chemical Function from a Few Good Reactions. *Angew. Chem., Int. Ed.* **2001**, *40*, 2004–2021.
- (3) Fleet, G. W. J.; Porter, R. R.; Knowles, J. R. Affinity Labelling of Antibodies with Aryl Nitrene as Reactive Group. *Nature* **1969**, *224*, 511–512.
- (4) Brase, S.; Gil, C.; Knepper, K.; Zimmermann, V. Organic azides: an exploding diversity of a unique class of compounds. *Angew. Chem., Int. Ed.* **2005**, *44*, 5188–5240.
- (5) Hein, C. D.; Liu, X. M.; Wang, D. Click chemistry, a powerful tool for pharmaceutical sciences. *Pharm. Res.* **2008**, *25*, 2216–2230.
- (6) Neves, A. A.; Stockmann, H.; Wainman, Y. A.; Kuo, J. C.; Fawcett, S.; Leeper, F. J.; Brindle, K. M. Imaging cell surface glycosylation in vivo using "double click" chemistry. *Bioconjugate Chem.* **2013**, *24*, 934–941.
- (7) Kiefer, H.; Lindstrom, J.; Lennox, E. S.; Singer, S. J. Photo-affinity labeling of specific acetylcholine-binding sites on membranes. *Proc. Natl. Acad. Sci. U. S. A.* **1970**, *67*, 1688–1694.

- (8) Nikic, I.; Kang, J. H.; Girona, G. E.; Aramburu, I. V.; Lemke, E. A. Labeling proteins on live mammalian cells using click chemistry. *Nat. Protoc.* **2015**, *10*, 780–791.
- (9) Hong, V.; Steinmetz, N. F.; Manchester, M.; Finn, M. G. Labeling live cells by copper-catalyzed alkyne–azide click chemistry. *Bioconjugate Chem.* **2010**, *21*, 1912–1916.
- (10) Poloukhine, A. A.; Mbuja, N. E.; Wolfert, M. A.; Boons, G. J.; Popik, V. V. Selective labeling of living cells by a photo-triggered click reaction. *J. Am. Chem. Soc.* **2009**, *131*, 15769–15776.
- (11) Laughlin, S. T.; Bertozzi, C. R. Metabolic labeling of glycans with azido sugars and subsequent glycan-profiling and visualization via Staudinger ligation. *Nat. Protoc.* **2007**, *2*, 2930–2944.
- (12) Vocadlo, D. J.; Hang, H. C.; Kim, E. J.; Hanover, J. A.; Bertozzi, C. R. A chemical approach for identifying O-GlcNAc-modified proteins in cells. *Proc. Natl. Acad. Sci. U. S. A.* **2003**, *100*, 9116–9121.
- (13) Speers, A. E.; Cravatt, B. F. Profiling enzyme activities in vivo using click chemistry methods. *Chem. Biol.* **2004**, *11*, 535–546.
- (14) Link, A. J.; Tirrell, D. A. Cell surface labeling of *Escherichia coli* via copper(I)-catalyzed [3 + 2] cycloaddition. *J. Am. Chem. Soc.* **2003**, *125*, 11164–11165.
- (15) Baskin, J. M.; Prescher, J. A.; Laughlin, S. T.; Agard, N. J.; Chang, P. V.; Miller, I. A.; Lo, A.; Codelli, J. A.; Bertozzi, C. R. Copper-free click chemistry for dynamic in vivo imaging. *Proc. Natl. Acad. Sci. U. S. A.* **2007**, *104*, 16793–16797.
- (16) Koo, H.; Lee, S.; Na, J. H.; Kim, S. H.; Hahn, S. K.; Choi, K.; Kwon, I. C.; Jeong, S. Y.; Kim, K. Bioorthogonal copper-free click chemistry in vivo for tumor-targeted delivery of nanoparticles. *Angew. Chem., Int. Ed.* **2012**, *51*, 11836–11840.
- (17) Birts, C. N.; Sanzone, A. P.; El-Sagheer, A. H.; Blaydes, J. P.; Brown, T.; Tavassoli, A. Transcription of click-linked DNA in human cells. *Angew. Chem., Int. Ed.* **2014**, *53*, 2362–2365.
- (18) Whiting, M.; Muldoon, J.; Lin, Y. C.; Silverman, S. M.; Lindstrom, W.; Olson, A. J.; Kolb, H. C.; Finn, M. G.; Sharpless, K. B.; Elder, J. H.; et al. Inhibitors of HIV-1 protease by using in situ click chemistry. *Angew. Chem., Int. Ed.* **2006**, *45*, 1435–1439.
- (19) Shelbourne, M.; Chen, X.; Brown, T.; El-Sagheer, A. H. Fast copper-free click DNA ligation by the ring-strain promoted alkyne–azide cycloaddition reaction. *Chem. Commun.* **2011**, *47*, 6257–6259.
- (20) Lewis, W. G.; Green, L. G.; Grynszpan, F.; Radic, Z.; Carlier, P. R.; Taylor, P.; Finn, M. G.; Sharpless, K. B. Click chemistry in situ: acetylcholinesterase as a reaction vessel for the selective assembly of a femtomolar inhibitor from an array of building blocks. *Angew. Chem., Int. Ed.* **2002**, *41*, 1053–1057.
- (21) El-Sagheer, A. H.; Sanzone, A. P.; Gao, R.; Tavassoli, A.; Brown, T. Biocompatible artificial DNA linker that is read through by DNA polymerases and is functional in *Escherichia coli*. *Proc. Natl. Acad. Sci. U. S. A.* **2011**, *108*, 11338–11343.
- (22) Shieh, P.; Siegrist, M. S.; Cullen, A. J.; Bertozzi, C. R. Imaging bacterial peptidoglycan with near-infrared fluorogenic azide probes. *Proc. Natl. Acad. Sci. U. S. A.* **2014**, *111*, 5456–5461.
- (23) Bharathi, M. V.; Chhabra, M.; Paira, P. Development of surface immobilized 3-azidocoumarin-based fluorogenic probe via strain promoted click chemistry. *Bioorg. Med. Chem. Lett.* **2015**, *25*, 5737–5742.
- (24) Lippert, A. R.; New, E. J.; Chang, C. J. Reaction-Based Fluorescent Probes for Selective Imaging of Hydrogen Sulfide in Living Cells. *J. Am. Chem. Soc.* **2011**, *133*, 10078–10080.
- (25) Lin, V. S.; Chang, C. J. Fluorescent probes for sensing and imaging biological hydrogen sulfide. *Curr. Opin. Chem. Biol.* **2012**, *16*, 595–601.
- (26) Lin, V. S.; Lippert, A. R.; Chang, C. J. Cell-trappable fluorescent probes for endogenous hydrogen sulfide signaling and imaging H₂O₂-dependent H₂S production. *Proc. Natl. Acad. Sci. U. S. A.* **2013**, *110*, 7131–7135.
- (27) Peng, H.; Cheng, Y.; Dai, C.; King, A. L.; Predmore, B. L.; Lefer, D. J.; Wang, B. A fluorescent probe for fast and quantitative detection of hydrogen sulfide in blood. *Angew. Chem., Int. Ed.* **2011**, *50*, 9672–9675.
- (28) Shieh, P.; Dien, V. T.; Beahm, B. J.; Castellano, J. M.; Wyss-Coray, T.; Bertozzi, C. R. CalFluors: A Universal Motif for Fluorogenic Azide Probes across the Visible Spectrum. *J. Am. Chem. Soc.* **2015**, *137*, 7145–7151.
- (29) Henthorn, H. A.; Pluth, M. D. Mechanistic Insights into the H₂S-Mediated Reduction of Aryl Azides Commonly Used in H₂S Detection. *J. Am. Chem. Soc.* **2015**, *137*, 15330–15336.
- (30) Kamali, F.; Gescher, A.; Slack, J. A. Medicinal azides. Part 3. The metabolism of the investigational antitumour agent meta-azidopyrimethamine in mouse tissue in vitro. *Xenobiotica* **1988**, *18*, 1157–1164.
- (31) Nicholls, D.; Gescher, A.; Griffin, R. J. Medicinal azides. Part 8. The in vitro metabolism of p-substituted phenyl azides. *Xenobiotica* **1991**, *21*, 935–943.
- (32) Pan-Zhou, X. R.; Cretton-Scott, E.; Zhou, X. J.; Yang, M. X.; Lasker, J. M.; Sommadossi, J. P. Role of human liver P450s and cytochrome b5 in the reductive metabolism of 3'-azido-3'-deoxythymidine (AZT) to 3'-amino-3'-deoxythymidine. *Biochem. Pharmacol.* **1998**, *55*, 757–766.
- (33) Kotra, L. P.; Manouilov, K. K.; Cretton-Scott, E.; Sommadossi, J. P.; Boudinot, F. D.; Schinazi, R. F.; Chu, C. K. Synthesis, biotransformation, and pharmacokinetic studies of 9-(beta-D-arabino-furanosyl)-6-azidopurine: a prodrug for ara-A designed to utilize the azide reduction pathway. *J. Med. Chem.* **1996**, *39*, S202–S207.
- (34) Elmes, R. B. Bioreductive fluorescent imaging agents: applications to tumour hypoxia. *Chem. Commun.* **2016**, *52*, 8935–8936.
- (35) Wilson, W. R.; Hay, M. P. Targeting hypoxia in cancer therapy. *Nat. Rev. Cancer* **2011**, *11*, 393–410.
- (36) Sun, W.; Fan, J.; Hu, C.; Cao, J.; Zhang, H.; Xiong, X.; Wang, J.; Cui, S.; Sun, S.; Peng, X. A two-photon fluorescent probe with near-infrared emission for hydrogen sulfide imaging in biosystems. *Chem. Commun.* **2013**, *49*, 3890–3892.
- (37) O'Connor, L. J.; Cazares-Korner, C.; Saha, J.; Evans, C. N.; Stratford, M. R.; Hammond, E. M.; Conway, S. J. Design, synthesis and evaluation of molecularly targeted hypoxia-activated prodrugs. *Nat. Protoc.* **2016**, *11*, 781–794.
- (38) Westerink, W. M.; Schoonen, W. G. Cytochrome P450 enzyme levels in HepG2 cells and cryopreserved primary human hepatocytes and their induction in HepG2 cells. *Toxicol. In Vitro* **2007**, *21*, 1581–1591.
- (39) Hammond, E. M.; Asselin, M. C.; Forster, D.; O'Connor, J. P.; Senra, J. M.; Williams, K. J. The meaning, measurement and modification of hypoxia in the laboratory and the clinic. *Clin. Oncol.* **2014**, *26*, 277–288.
- (40) Yasui, H.; Matsumoto, S.; Devasahayam, N.; Munasinghe, J. P.; Choudhuri, R.; Saito, K.; Subramanian, S.; Mitchell, J. B.; Krishna, M. C. Low-field magnetic resonance imaging to visualize chronic and cycling hypoxia in tumor-bearing mice. *Cancer Res.* **2010**, *70*, 6427–6436.
- (41) Pires, I. M.; Bencokova, Z.; Milani, M.; Folkes, L. K.; Li, J. L.; Stratford, M. R.; Harris, A. L.; Hammond, E. M. Effects of acute versus chronic hypoxia on DNA damage responses and genomic instability. *Cancer Res.* **2010**, *70*, 925–935.
- (42) Costes, S. V.; Daelemans, D.; Cho, E. H.; Dobbin, Z.; Pavlakis, G.; Lockett, S. Automatic and quantitative measurement of protein–protein colocalization in live cells. *Biophys. J.* **2004**, *86*, 3993–4003.
- (43) Manders, E. M. M.; Verbeek, F. J.; Aten, J. A. Measurement of colocalization of objects in dual-colour confocal images. *J. Microsc.* **1993**, *169*, 375–382.
- (44) Cazares-Korner, C.; Pires, I. M.; Swallow, I. D.; Grayer, S. C.; O'Connor, L. J.; Olcina, M. M.; Christlieb, M.; Conway, S. J.; Hammond, E. M. CH-01 is a Hypoxia-Activated Prodrug That Sensitizes Cells to Hypoxia/Reoxygenation Through Inhibition of Chk1 and Aurora A. *ACS Chem. Biol.* **2013**, *8*, 1451–1459.
- (45) Wardman, P. Reduction Potentials of One-Electron Couples Involving Free-Radicals in Aqueous-Solution. *J. Phys. Chem. Ref. Data* **1989**, *18*, 1637–1755.
- (46) Wardman, P.; Rothkamm, K.; Folkes, L. K.; Woodcock, M.; Johnston, P. J. Radiosensitization by nitric oxide at low radiation doses. *Radiat. Res.* **2007**, *167*, 475–484.
- (47) O'Neill, P.; Wardman, P. Radiation chemistry comes before radiation biology. *Int. J. Radiat. Biol.* **2009**, *85*, 9–25.

(48) Meng, F.; Evans, J. W.; Bhupathi, D.; Banica, M.; Lan, L.; Lorente, G.; Duan, J. X.; Cai, X.; Mowday, A. M.; Guise, C. P.; Maroz, A.; Anderson, R. F.; Patterson, A. V.; Stachelek, G. C.; Glazer, P. M.; Matteucci, M. D.; Hart, C. P. Molecular and cellular pharmacology of the hypoxia-activated prodrug TH-302. *Mol. Cancer Ther.* **2012**, *11*, 740–751.

(49) Wardman, P.; Priyadarsini, K. I.; Dennis, M. F.; Everett, S. A.; Naylor, M. A.; Patel, K. B.; Stratford, I. J.; Stratford, M. R.; Tracy, M. Chemical properties which control selectivity and efficacy of aromatic N-oxide bioreductive drugs. *Br. J. Cancer Suppl.* **1996**, *27*, S70–74.

(50) Jaffar, M.; Everett, S. A.; Naylor, M. A.; Moore, S. G.; Ulhaq, S.; Patel, K. B.; Stratford, M. R.; Nolan, J.; Wardman, P.; Stratford, I. J. Prodrugs for targeting hypoxic tissues: regiospecific elimination of aspirin from reduced indolequinones. *Bioorg. Med. Chem. Lett.* **1999**, *9*, 113–118.

(51) Takano, N.; Peng, Y. J.; Kumar, G. K.; Luo, W.; Hu, H.; Shimoda, L. A.; Suematsu, M.; Prabhakar, N. R.; Semenza, G. L. Hypoxia-inducible factors regulate human and rat cystathionine beta-synthase gene expression. *Biochem. J.* **2014**, *458*, 203–211.

(52) Farwell, C. C.; McIntosh, J. A.; Hyster, T. K.; Wang, Z. J.; Arnold, F. H. Enantioselective Imidation of Sulfides via Enzyme-Catalyzed Intermolecular Nitrogen-Atom Transfer. *J. Am. Chem. Soc.* **2014**, *136*, 8766–8771.

(53) Singh, R.; Bordeaux, M.; Fasan, R. P450-catalyzed intramolecular C-H amination with arylsulfonyl azide substrates. *ACS Catal.* **2014**, *4*, 546–552.

(54) Sasmal, P. K.; Carregal-Romero, S.; Han, A. A.; Streu, C. N.; Lin, Z.; Namikawa, K.; Elliott, S. L.; Koster, R. W.; Parak, W. J.; Meggers, E. Catalytic azide reduction in biological environments. *ChemBioChem* **2012**, *13*, 1116–1120.

(55) Pires, I. M.; Olcina, M. M.; Anbalagan, S.; Pollard, J. R.; Reaper, P. M.; Charlton, P. A.; McKenna, W. G.; Hammond, E. M. Targeting radiation-resistant hypoxic tumour cells through ATR inhibition. *Br. J. Cancer* **2012**, *107*, 291–299.